Availability Assessment Based Case-Sensitive Power System Restoration Strategy

Weijia Liu, Junpeng Zhan, *Member, IEEE*, C. Y. Chung, *Fellow, IEEE*, and Lei Sun

***Abstract* — Increasingly frequent severe weather events in recent years threaten the security of power systems and result in major power outages throughout the world. The development of reasonable power system restoration (PSR) solutions is therefore urgently needed to speed up the recovery of the power supply while at the same time steering clear of vulnerable and risky equipment. This paper aims to develop a case-sensitive PSR model for power transmission systems that can adjust restoration solutions according to the evaluated availability of outage equipment in specific blackout scenarios and weather conditions. A novel PSR model that integrates the startup of generating units, formulation of the restoration network, renewable energy sources, and availability assessment of devices is proposed. A reformulated model is also proposed to relieve the computational burden of complex PSR problems. The availability of outage equipment is comprehensively assessed based on historical operating records, fault diagnosis results, and weather conditions. The assessed availability results are sensitive to the characteristics of real blackout cases and will support system operators generate case-sensitive PSR solutions while mitigating the vulnerable equipment. The feasibility and effectiveness of the proposed PSR model and its reformulations are verified through case studies.**

***Index Terms* — Fault diagnosis, power system restoration, power system resilience, availability assessment**

NOMENCLATURE

Sets

$\Omega_{\mathrm{A}(x)}$	Set of alarms related to device *x*
Ω_{L}	Set of power lines in blackout area
Ω_{N}	Set of buses in blackout area
Ω_{T}	Set of time slots
Ω_{X}	Set of devices in blackout area
Ω_{Y}	Set of severe weather factors

Parameters

b_{ij}, b_{ij}^{lc}	Series and shunt susceptance of line *ij*
g_{ij}	Series conductance of line *ij*
N_{B}	Number of blackout buses
N_{L}	Number of blackout lines
N_{T}	Number of considered time slots
$P_{i,t}^{\mathrm{G,est}}$	Forecasted active power generation capacity for renewable energy source at bus *i* at time *t*
P_i^{set}	Active power rating of the non-black-start power plant at bus *i*
P_i^{L}	Startup load of power plant at bus *i*
P_i^{rp}	Ramping rate of power plant at bus *i*
Q_i^{L}	Reactive load at bus *i*
τ_i^{st}	Required time to start ramping of the non-black-start power plant at bus *i*
τ_i^{rp}	Total ramping time of non-black-start power plant at bus *i* to reach P_i^{set}
ϖ_i^{lim}	Power factor limit of renewable energy sources
η_i	Reserve margin of renewable energy forecasts
$\Delta\tau_{ij}$	Required time to restore line *ij*

Variables

d_a	Received alarm signal
$d_a^{h_x}$	Expected alarm signal based on fault hypothesis
f_x	Availability of device *x* based on fault diagnosis
h_x	Fault hypothesis for device *x*
$P_{i,t}$	Active nodal power injection at bus *i* at time *t*
$P_{i,t}^{\mathrm{G}}$	Active power generation capacity at bus *i* at time *t*
$P_{i,t}^{\mathrm{L}}$	Active power load at bus *i* at time *t*
$P_{ij,t}$	Active power flow through line *ij* at time *t*
$Q_{i,t}$	Reactive nodal power injection at bus *i* at time *t*
$Q_{i,t}^{\mathrm{G}}$	Reactive power generation at bus *i* at time *t*
$Q_{i,t}^{\mathrm{L}}$	Reactive power load at bus *i* at time *t*
$Q_{ij,t}$	Reactive power flow through line *ij* at time *t*
$\Delta Q_{i,t}^{\mathrm{lc}}$	Nodal reactive power increment of restoring line *ij* at time *t*
r_x	Availability assessment of device *x* based on historical operating records
s_x	Availability assessment of device *x* against severe weather events
$s_{x,y}$	Survivability of device *x* against environmental factor *y*
$V_{i,t}$	Nodal voltage magnitude of bus *i* at time *t*
$v_{x,y}$	Impact of environmental factor *y* on device *x*
$v_{x,y}^{\mathrm{std}}$	The designed standard of device *x* against the environmental factor *y*
$\alpha_{i,t}$	Restoration status of bus *i* at time *t*
$\beta_{i,t}$	Ramping status of the non-black-start power plant at bus *i* at time *t*
$\gamma_{ij,t}$	On-off status of line *ij* at time *t*
$\theta_{i,t}$	Nodal voltage phase angle of bus *i* at time *t*
ϑ_i	Restored time of bus *i*
ξ_{ij}	The indicator of restoration direction of line *ij*
μ_i	On/off status of bus *i*
ω	The weighting factor of fault diagnosis results
$\varphi_{ij,t}^{\mathrm{p}}$, $\varphi_{ij,t}^{\mathrm{q}}$	Ancillary variable for active and reactive power flow of line *ij* at time *t*

The work was supported in part by the Natural Sciences and Engineering Research Council (NSERC) of Canada and the Saskatchewan Power Corporation (SaskPower). This work was authored in part by the National Renewable Energy Laboratory, operated by Alliance for Sustainable Energy, LLC, for the U.S. Department of Energy (DOE) under Contract No. DE-AC36-08GO28308.

W. Liu is with the Department of Electrical and Computer Engineering, University of Saskatchewan, Saskatoon, SK S7N 5A9, Canada, and also with the Power System Engineering Center, National Renewable Energy Laboratory, Golden, CO 80401, U.S.A. (e-mail: liuweijiamarcel@gmail.com).

J. Zhan is with the Department of Electrical and Computer Engineering, University of Saskatchewan, Saskatoon, SK S7N 5A9, Canada, and also with the Sustainable Energy Technologies Department, Brookhaven National Laboratory, Upton, NY 11973, U.S.A. (e-mail: zhanjunpeng@gmail.com)

C. Y. Chung is with the Department of Electrical and Computer Engineering, University of Saskatchewan, Saskatoon, SK S7N 5A9, Canada. (e-mail: c.y.chung@usask.ca).

Lei Sun is with the School of Electrical Engineering and Automation, Hefei University of Technology, Hefei 230009, China. (e-mail: leisun@hfut.edu.cn).

ψ_x, ψ_x^-	Evaluated availability and risk indexes of device x
$\Psi_{\sum x}$	Integrated availability index of restoring a set of devices
Ψ_i, Ψ_i^-	Evaluated cumulative availability and risk indexes to restore bus i
Superscripts	
min/max	Minimum or maximum limit of a quantity

I. Introduction

BLACKOUTS threaten the security of electricity supply and incur enormous social and economic damage around the world. Although the resilience of modern power grids has been enhanced with the implementation of advanced monitoring and control systems, blackouts cannot be fully averted due to the vulnerabilities of transmission and distribution facilities, especially in cases of severe weather events [1,2]. According to a recent survey, the majority of recent blackouts have been weather-related [3]. For example, a disastrous winter storm caused a major blackout in southern China in 2008, disturbing the power supply for over 25 million people [4]. Hurricane Sandy struck the U.S. in 2012 and resulted in power outages for more than 8.5 million households and businesses [5]. The major blackout of South Australia in 2016 that affected around 1.7 million people was also caused by a severe storm [6]. Effective strategies to restore power supply after such disastrous events are in urgent need to reduce the negative influences of blackouts on economy and society.

The restoration of power supply after blackouts is generally referred to as power system restoration (PSR), the strategy of which plays a key role in directing the recovery steps and the implementation of black-start resources. After a blackout, the black-start units (BSUs) that can start on their own without external power supply are the power sources to initiate the PSR [1]. Substations and transmission lines will be energized to create a cranking path for the BSUs to supply cranking power to the non-black-start units (NBSUs) that rely on the external power supply to start. With sufficient generating units back up online, the load supply will be gradually recovered to finalize the PSR process.

With the ever-growing threats from extreme weather events, the development of reasonable PSR strategy for weather-related blackouts becomes crucial because severe weather not only triggers blackouts by causing permanent or long-term faults but also threatens the proper functioning of power system facilities. Motivated by the inevitable need to restore the power supply after weather-related blackouts, this paper investigates the modeling of PSR that are capable of identifying the causes of specific blackouts and properly handling potential risk factors (e.g., faulted devices, equipment that might suffer from severe weather conditions) to secure the success of system recovery in a timely fashion.

A. Literature Review

The PSR is usually divided into three stages—the startup of NBSUs, the formulation of restoration networks/islands, and the restoration of power loads [7]—each of which has been separately studied in the existing literature. For the first stage, a fuzzy decision-making support method is proposed in [7] to obtain the optimal black-start scheme based on selected key factors. The NBSU restoration strategy to supply cranking power to NBSUs is optimized in [8] considering the startup characteristics of NBSUs. The steam-turbine cylinder temperature of NBSUs is also estimated in [9] to enhance the efficiency and feasibility of unit startup decisions. These studies generally emphasize the optimization of NBSU startup sequences based on the status of NBSUs, while the formulations of cranking paths and restoration networks/islands are generally simplified or ignored. For the second stage, the allocation of BSUs and the division of islands are optimized in [10] from the viewpoint of cost-efficiency. Alternatively, a blackout system can be divided into several islands and restored in parallel by different BSUs to speed up the restoration process. These islands are referred to as restoration islands in the rest of the paper, and the topology information is used to generate the parallel restoration islands in [11]. The configuration of restoration networks is generated based on graph theory and a self-healing algorithm is derived in [12]. The restoration strategies of microgrid-based distribution systems and unbalanced distributions systems are respectively developed in [13] and [14]. The similar aims of these research works are to generate an optimal backbone network to assist the PSR process, but the startup and ramping characteristics of NBSUs have not been sophisticatedly considered. For the third stage, an optimization load restoration scheme in transmission systems considering power system dynamics is proposed in [15]. The critical load restoration problem in distribution systems is studied in [16]. The present paper focuses on the first two stages. Load restoration is not further discussed because most generating units and transmission lines have already been synchronized at the load restoration stage, making it less complex compared to the other two stages.

Summarized from the literature review, several weaknesses of existing PSR studies can be identified:

1) Different PSR stages have not been comprehensively integrated. In the aforementioned research [7]-[16], the cranking of NBSUs and the formulation of restoration network are separately modeled and analyzed. Efforts have been made in studies such as [17] and [18] to coordinate multiple PSR stages, but the startup of NBSUs remains the dominant stage. Once the startup sequences of NBSUs are optimized, the configuration of the restoration network can be accordingly obtained. However, the startup of NBSUs can only be accomplished by restoring certain transmission lines, while energizing lightly loaded transmission lines requires support from available generating units. It turns out that, the startup of NBSUs and the formulation of restoration network are deeply coupled during a PSR process. Moreover, if transmission infrastructure fails to construct the backbone network due to factors such as faults and extreme weather, the optimized startup sequence of NBSUs cannot be achieved. Thus, the interactions between these two PSR stages should be respected and comprehensively integrated when formulating PSR models.
2) In existing PSR studies, the emphasis is laid on the planning and optimization of universal PSR solutions that assume the availability of most transmission/distribution facilities and do not distinguish the characteristics of different blackout cases (e.g., reasons that caused the blackouts and potential threats to the success of PSR). In this paper, these studies are categorized as *case-insensitive* because their PSR solutions cannot be adjusted with respect to specific blackout cases, especially those related to severe weather. In cases of weather-related blackouts, existing case-insensitive PSR solutions might lead to the restoration of lines and substations that suffer from faults or severe weather, which introduces excessive risks to the PSR and threatens the success of NBSU startup and restoration network formulation.
3) The positive role of renewable energy sources (RESs) in accelerating the PSR process has not been explored in depth. The fast-growing capacity and black-start capability make it possible for RESs to act as black-start units (BSUs) and contribute to the PSR [19]-[21]. Meanwhile, the uncertainty of

RESs will introduce great difficulties in planning the PSR solutions, especially for existing case-insensitive PSR models. On the one hand, uncertainty modeling methods such as stochastic optimization significantly boost the computational burden. On the other hand, the generation outputs of RESs may deviate significantly from their schedules because the case-insensitive PSR solutions are generated way ahead of the occurrence of the actual blackout, meaning that existing case-insensitive PSR models with RESs may result in over-optimistic or over-pessimistic solutions.

B. Proposed Approaches

To tackle these weaknesses, this paper attempts to propose a *case-sensitive* PSR strategy that not only integrates the startup sequence optimization of NBSUs and the formulation of restoration networks but also alleviates unnecessary risks introduced by restoring devices that suffer from faults or severe weather. In comparison to existing case-insensitive PSR studies, the case-sensitivity is defined as the capability to automatically generate PSR solutions considering the characteristics of specific blackout cases including fault information, weather influences, etc. The case-sensitive PSR model developed here also accommodates the integration of RESs, whose uncertainty factors can be well monitored through short-term forecasts that fit the proposed case-sensitive context. Unlike existing PSR planning models that optimize PSR strategies with simulated blackout cases, the proposed case-sensitive PSR model generate PSR solutions soon after the occurrence of a major outage to support system operators in decision-making with respect to the characteristics of the specific blackout.

To achieve this, three major obstacles are addressed. The first is to build a connection between NBSU startup and network restoration. The key variable in the first stage is the startup timing information of NBSUs, while the second stage aims to optimize the on/off statuses of transmission lines/substations. Therefore, a reasonable connection must be found between NBSU startup and network restoration, and this connection should be modeled properly so that the mathematical models of these two stages can be integrated. The second is to properly assess the availability of transmission equipment to alleviate the restoration of risky devices, and further integrate the availability assessment results into the PSR model. In addition to the consideration of specific blackout cases, a desirable case-sensitive PSR solution should be made available to system operators as fast as possible after the occurrence of the blackouts to minimize the negative influences of blackouts. Hence, the third obstacle is to effectively solve the PSR model so that the system operators are able to make case-sensitive decisions after the blackout occurs. Besides, enhancing computational efficiency also greatly eliminates the negative impacts of RES generation uncertainties since the short-term RES generation forecasts are more accurate compared to long-term ones.

In this paper, the connection between NBSU startup and network restoration is constructed based on graph theory, and the power flow constraints of the dynamic restoration network are linearized and integrated into the PSR model to guarantee the feasibility of optimized PSR solutions. To relieve the computational burden of the proposed PSR model and effectively utilize the short-term RES generation forecasts, a reformulation model is developed. The availability of transmission facilities will be comprehensively assessed by consulting multiple data sources, including historical operating records, fault diagnosis results, and geography-related weather conditions. The assessment indices can reflect the success rate of restoring certain lines/substations with respect to the specific blackout cases.

C. Contributions and Paper Organization

The contributions of this paper are summarized as follows.

1. The availability of power equipment after blackouts is defined, with a special emphasis laid on weather-related blackouts. A novel comprehensive availability assessment method is proposed to evaluate the success rate of restoration operation based on post-blackout data. The available power generation of RESs is also integrated into the availability assessment module. Instead of introducing complex uncertainty modeling, the short-term RES forecasts are valid within the proposed case-sensitive PSR context.
2. A novel integrated PSR model (referred to as the full model) is proposed to overcome the research lap in coordinating the startup sequence optimization of NBSUs and the formulation of a restoration backbone network. As such, the proposed PSR model provides holistic PSR solutions that cannot be delivered by existing literature to date.
3. A novel reformulated model is developed to simplify the time-consuming power flow constraints. The reformulated model can boost the PSR model solution process to make sure that system operators are able to quickly make case-sensitive decisions after blackouts without violating power system operating constraints. The assessed availability is also properly integrated into both the full and reformulated models so that case-sensitive PSR solutions can be obtained.

The remainder of the paper is organized as follows. The framework of the proposed case-sensitive PSR strategy is described in Section II. Section III discusses the availability assessment of transmission equipment. Section IV proposes the full PSR model that integrates the startup of NBSUs, network reconfiguration, and power flow constraints. To relieve the computational burden, a novel reformulated model is also developed in Section IV. Section V integrates availability assessment into the proposed PSR models. The effectiveness of proposed PSR models is validated through case studies in Section VI. Finally, conclusions are drawn in Section VII.

II. Problem Overview

The main principle of PSR is to recover power supply to customers as fast as possible to reduce the negative influences of power outages. To recover from a blackout, power system operators are required to arrange the cranking of generating units and energize a backbone network to stabilize the fundamental restored system, which is also the emphasis of this paper. This process is demonstrated in Fig. 1(a). In Fig. 1(a), three NBSUs with priorities ‘1’>’2’>’3’ will be restored by the BSU denoted by ‘B’. More transmission buses/lines and power loads will have faster access to the power supply after the restored system becomes strong enough.

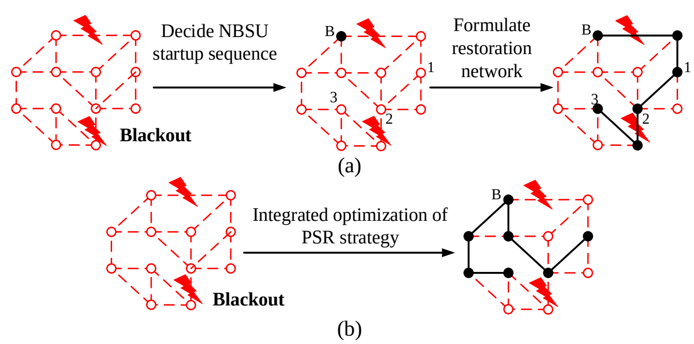

Fig. 1. Diagram of PSR process: (a) case-insensitive PSR that does not integrate NBSU startup and network configuration; (b) proposed case-sensitive PSR.

Although power companies generally have generalized PSR plans to deal with imaginary blackout scenarios, the feasibility of those case-insensitive plans cannot be guaranteed, especially in cases of extreme events. Take the illustration in Fig. 1(a) as an example, if some cranking paths to the NBSUs are damaged (i.e., lines with lightening signs), the restoration plan denoted by solid lines in Fig. 1(a) becomes infeasible. Thus, the desired restoration plan should integrate the NBSU startup and network configuration to ensure the feasibility and case sensitivity, as shown in Fig. 1(b).

To achieve case sensitivity in PSR shown in Fig. 1(b), the system operators shall optimize the restoration strategies after the occurrence of a blackout. After gathering necessary information regarding the cause and impact of the power outage, the system operator will evaluate available resources and construct a PSR solution that corresponds to the characteristics of the specific blackout case. A flowchart illustrating the proposed PSR process is shown in Fig. 2. Note that all the modules in Fig. 2 are within the scope of the power system operator. In addition to the mathematical models to optimize PSR solutions, the key to enabling the case sensitivity is the availability assessment module in Fig. 2. In this paper, the availability of a transmission component is defined as its success rate to be energized after an outage (e.g., energizing transmission lines and substations). The evaluation of availability is discussed in detail in Section III.

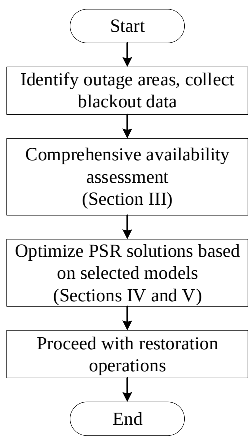

Fig. 2. Flowchart of the proposed PSR method.

III. Comprehensive Assessment of Power Equipment and RES Generation Availability

The transmission/distribution facilities, e.g., substations and transmission lines, are generally assumed to be available in conventional PSR studies. However, the restoration of fault facilities can introduce significant disturbances that are intolerable for the newly restored system. Thus, the availability of power equipment in outage areas should be comprehensively evaluated so that the restoration of vulnerable and risky facilities can be alleviated. In addition, the available power generation of RESs is also included in the proposed availability assessment module.

A flowchart of the proposed availability assessment module is shown in Fig. 3. Both offline and online assessments are employed and integrated to assess the availability of transmission facilities and the available generation capacity of RESs. Furthermore, it is assumed that both offline and online data are accessible to the system operators after the blackout.

A. Offline Reliability Assessment Module

The offline reliability assessment module aims to evaluate the statistical reliabilities of transmission equipment based on historical operating records derived from an offline database. In this paper, the reliability of power equipment is represented by the forced outage rate (FOR), which is widely used in power system reliability studies. Let $1-r_x$ denote the FOR of equipment x. The calculation of FOR can be found in [22] and [23], the evaluated FOR of outage equipment is assumed to be available to the system operator when a blackout occurs. r_x is the output index for this offline availability assessment module and is case-insensitive.

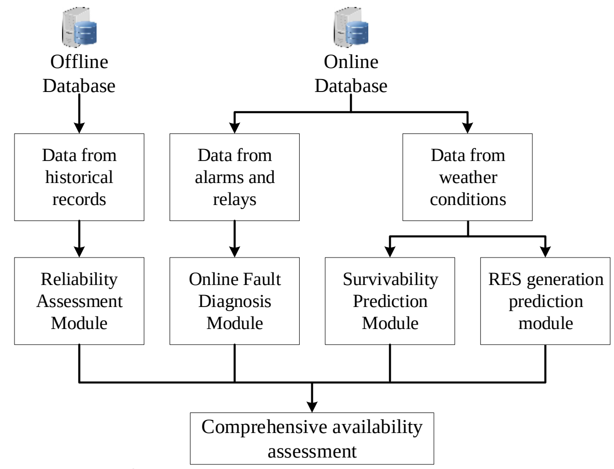

Fig. 3. Flowchart of availability assessment module.

B. Online Fault Diagnosis Module

Generally, faults are the direct cause of power system blackouts. When faults occur, the protective relays will function to protect the security of power system facilities based on alarm signals. Facilities that have suffered from failures are considered more vulnerable and should not be prioritized during restoration. However, a single fault might result in numerous alarm signals and the tripping of multiple circuit breakers. Modern fault diagnosis methodologies are able to identify the fault devices based on alarm information derived from an online database and predefined logics of protection relays. An analytic diagnosis model proposed in [24] and [25] is adopted to identify fault facilities, which is briefly described as follows:

Let $\mathbf{H_x}=\{h_x|x\in\Omega_X\}$ denote a fault hypothesis of devices in the outage area, where $h_x=1$ and 0 correspond to the faulted and normal states of device x, respectively. The fault diagnosis model aims to find the hypothesis that is the most consistent with the operation logic of received alarms. In general, the fault diagnosis can be expressed by the following model:

$$\text{Min } \sum_{x\in\Omega_{\mathrm{X}}}\sum_{a\in\Omega_{\mathrm{A}(x)}}|d_a-d_a^{h_x}| \tag{1}$$

Equation (1) minimizes the inconsistency between the fault hypothesis and received alarms. $d_a^{h_x}$ denotes the expected set of alarms if hypothesis h_x is true, and can be derived from the logic reasoning of installed protective relays.

The adopted analytic fault diagnosis model can be efficiently solved by a Tabu search algorithm, which generally takes a few seconds to obtain the most reasonable hypotheses and identify faulted facilities [25]. Typically, the faulted devices should not be restored for security concerns, but some devices might suffer from temporary faults or disturbances and are actually available for restoration. Thus, the identified faulted devices are given lower priorities in the PSR process based on the risk preference of system operator. For example, a weighting factor $\omega\in[0,1]$ can be adopted to represent the preferences of system operators:

$$f_x=1-\omega h_x \tag{2}$$

where f_x is the output index for fault diagnosis and can be calculated based on the optimized fault hypothesis h_x. If x is identified as a faulted device ($h_x=1$), f_x equals $1-\omega$. Otherwise, x is not considered to be faulted and the corresponding availability f_x

equals 1. By increasing (decreasing) the value of ω, a more risk-averse (risk-seeking) f_x will be obtained from (2) to accommodate the risk preferences of the system operator.

C. Online Survivability Prediction Module

The operation of power system facilities is influenced by factors such as temperature and humidity, and the impacts of these environmental factors should be considered more seriously in cases of weather-related blackouts. Facilities that have suffered or will suffer from severe weather are exposed to higher risks of malfunction, which should be properly considered during PSR.

To evaluate the survivability of power equipment encountering a severe weather event, a number of environmental factors can be identified as key factors according to the features of the specific weather event concerned. For example, wind speed and freezing precipitation are chosen as key factors in cases of ice storms or freezing rain. For any facility *x* and a given environmental factor *y*, *x* is believed to withstand *y* if the value of the environmental factor (denoted as $v_{x,y}$) is within the designed standard of *x*, denoted as $v_{x,y}^{\text{std}}$. If $v_{x,y}$ is beyond $v_{x,y}^{\text{std}}$, then *x* becomes vulnerable to *y*. As a commonly used method in extreme value analysis and a special case of generalized Pareto distribution [26], the cumulative distribution function of the exponential distribution shown in (3) is adopted to evaluate the survivability of device *x* against environmental factor *y* (denoted as $s_{x,y}$):

$$s_{x,y} = \begin{cases} 1 & , \ v_{x,y} \le v_{x,y}^{\text{std}} \\ e^{-\varepsilon_{x,y}(v_{x,y}/v_{x,y}^{\text{std}}-1)}, & v_{x,y} > v_{x,y}^{\text{std}} \end{cases} \tag{3}$$

where $s_{x,y}$ decreases exponentially as $v_{x,y}$ grows larger than $v_{x,y}^{\text{std}}$. In practice, $v_{x,y}$ is measured and forecasted by related authorities and is assumed to be accessible to system operators. The parameter $\varepsilon_{x,y}$ can be obtained by introducing an additional set of data. For example, the survivability of *x* in case of an extreme condition $v_{x,y}^{*}$ is estimated as $s_{x,y}^{*}$, then $\varepsilon_{x,y}$ is calculated using

$$\varepsilon_{x,y} = -\frac{v_{x,y}^{\text{std}}}{v_{x,y}^{*}-v_{x,y}^{\text{std}}} \ln\left(s_{x,y}^{*}\right) \tag{4}$$

Note that the data set $\{v_{x,y}^{*}, s_{x,y}^{*}\}$ also reflects the risk preferences of system operators in terms of equipment survivability against extreme weather. For example, if $s_{x,y}^{*}$ is approximated to be 1% (0.1%) at $v_{x,y}^{*} = 2v_{x,y}^{\text{std}}$, then $\varepsilon_{x,y}$ equals 4.6 (6.9). Thus, higher $\varepsilon_{x,y}$ indicates that the system operator tends to be more conservative in estimating the equipment survivability.

As a result, the availability of *x* can be derived from the predicted survivability of *x* influenced by different environmental factors, which is given by

$$s_x = \prod_{y\in\Omega_{\text{Y}}} s_{x,y} \tag{5}$$

D. Availability of RES Power Generation

In conventional PSR planning problems, stochastic optimization methods are widely employed to generate robust and conservative PSR solutions with RESs long before a blackout happens [20]. Another solution is to introduce energy storage units as a complementary resource for the intermittent RESs in the PSR process, the feasibility of which is validated by our previous work [21] and [27] and will not be further discussed in this paper. In conclusion, RESs are integrated into restoration models to generate case-insensitive solutions in existing research.

In the proposed case-sensitive PSR context, the restoration strategies are optimized after the blackout occurs. Thus, the short-term RES forecasts that usually last for a few hours but have high accuracy can be employed by the system operators, as shown in Fig. 3. Since the short-term RES forecast technique is not the contribution of this paper and has been extensively studied in existing literature such as [28]. In this paper, it is assumed that the short-term RES generation forecasts are available to system operators. The following constraints are employed to constrain the power output of RESs during restoration.

$$0 \le P_{i,t}^{\text{G}} \le \eta_i P_{i,t}^{\text{G,est}} \tag{6}$$

$$Q_{i,t}^{\text{G}} \le \tan(\cos^{-1}\varpi_i^{\text{lim}})\, P_{i,t}^{\text{G}} \tag{7}$$

$$Q_{i,t}^{\text{G}} \ge -\tan(\cos^{-1}\varpi_i^{\text{lim}})\, P_{i,t}^{\text{G}} \tag{8}$$

The active power of RES is constrained by (6), the reserve margin η_i is introduced to accommodate possible forecast errors of RES generation outputs. Constraints (7) and (8) are derived from [29] to represent the reactive power output limits of RESs.

Note that the short-term forecast errors are ignored due to the following two considerations:

(i) The RES generation forecast error generally grows considerably with the increase in forecast time length [30]. The short-term forecast with a forecast timescale of a few hours has the highest forecast accuracy (e.g., the typical forecast error of a modern wind farm is less than 10% in 12 hours ahead [31]). Thus, it is reasonable to ignore the short-term forecast error. Risk-averse operators can also utilize more conservative forecasts (e.g., set $\eta_i = 0.9$ to accommodate 10% forecast errors) at their own preference.

(ii) Acting as BSUs, the key role of RESs is to provide cranking power to NBSUs, especially in the first few hours after the blackout when the active power generation capacity is scarce. As mentioned above, the forecast error generally grows as the increase in forecast time length, which indicates that the error of short-term RES generation forecasts may gradually increase as the PSR process proceeds. Nonetheless, the restoration and ramping of NBSUs will take the place of RESs to produce active power. Thus, the influence of larger RES forecast errors in the latter stage of a PSR process is not significant.

IV. Integrated Power System Restoration Model and Its Reformulation

A. Integrated Power System Restoration Model – Full Model

The first two stages of the PSR process normally share a common target, i.e., maximizing the net active power generation capacity. The objective function of the PSR model can be described as:

$$\text{Max} \ \sum_{i\in\Omega_{\text{N}}}\sum_{t\in\Omega_{\text{T}}}(P_{i,t}^{\text{G}} - P_{i,t}^{\text{L}}) \tag{9}$$

The net active power generation capacity profile of a typical NBSU is described in Fig. 4(a), which can be decomposed into a power output curve and an auxiliary power consumption curve as illustrated in Figs. 4(b) and 4(c), respectively.

The active power generation capacity is decided by the generator startup sequences, and can be modeled as follows:

$$0 \le P_{i,t}^{\text{G}} \le \beta_{i,t}(P_i^{\text{set}} + P_i^{\text{L}}) \tag{10}$$

$$\beta_{i,t}Q_i^{\text{G,min}} \le Q_{i,t}^{\text{G}} \le \beta_{i,t}Q_i^{\text{G,max}} \tag{11}$$

$$P_{i,t}^{\text{L}} - \alpha_{i,t}P_i^{\text{L}} = 0 \ , \ Q_{i,t}^{\text{L}} - \alpha_{i,t}Q_i^{\text{L}} = 0 \tag{12}$$

$$P_{i,t}^{\text{G}} - P_{i,t-1}^{\text{G}} - \beta_{i,t}P_i^{\text{rp}} \le 0 \tag{13}$$

$$\vartheta_i - \sum_{t\in\Omega_{\text{T}}}(1-\alpha_{i,t}) = 0 \tag{14}$$

$$\vartheta_i^{\min} \le \vartheta_i \le \vartheta_i^{\max} \tag{15}$$

$$\vartheta_i + \tau_i^{\text{st}} + 1 - \sum_{t\in\Omega_{\text{T}}}\left(1-\beta_{i,t}\right) = 0 \tag{16}$$

$$\alpha_{i,t-1} - \alpha_{i,t} \le 0 \ , \beta_{i,t-1} - \beta_{i,t} \le 0 \tag{17}$$

$$\alpha_{i,t}, \beta_{i,t} \in \{0,1\} \tag{18}$$

Equations (10)-(12) constrain the nodal active/reactive power generation and consumption, (13) constrains the ramping process of the NBSUs, (14) calculates the restoration time of NBSUs and is further constrained by the corresponding minimum and maximum restoration intervals in (15), the time that NBSUs start ramping is calculated in (16), and the binary variables $\alpha_{i,t}$ and $\beta_{i,t}$ are constrained by (17) and (18). Note that $P_{i,t}^{\mathrm{G}}$ denotes the available power generation capacity that represents the maximum power output based on the restoration status, not the actual active power output. The actual power generation output also depends on the coordination of load restoration, which will be discussed in the power flow constraints.

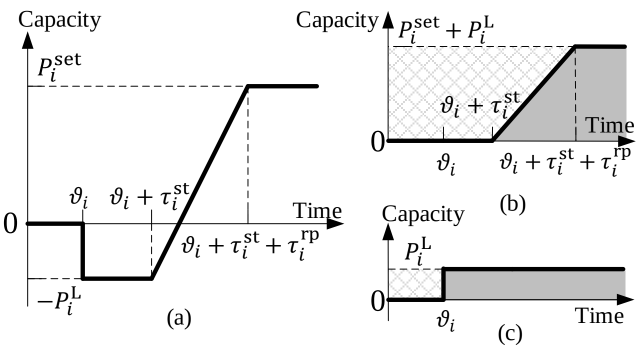

Fig. 4. Typical generation capacity curve of an NBSU: (a) net generation capacity ($P_{i,t}^{\mathrm{G}} - P_{i,t}^{\mathrm{L}}$), (b) output capacity ($P_{i,t}^{\mathrm{G}}$), and (c) startup and auxiliary power consumption ($P_{i,t}^{\mathrm{L}}$).

The restoration timestamp ϑ_i is the most important variable in the NBSU startup sequence modeled in (10)-(18). At the same time, ϑ_i is also influenced by the cranking paths and the formation of the restoration network. Because each blackout bus can be restored from one of its adjacent buses by energizing the transmission line connecting them, constraints (19)-(25) are proposed to build the connections between the restoration network and ϑ_i.

$$\xi_{ij} + \xi_{ji} \le 1 \tag{19}$$

$$\textstyle\sum_{ij\in\Omega_{\mathrm{L}}} \xi_{ji} - \mu_i = 0 \tag{20}$$

$$0 \le \mu_i \le 1 \tag{21}$$

$$M(1-\mu_i) - \vartheta_i \le 0 \tag{22}$$

$$\vartheta_i - \vartheta_j + \Delta\tau_{ij} - M\big(1-\xi_{ij}\big) \le 0 \tag{23}$$

$$\vartheta_j - \vartheta_i + \Delta\tau_{ij} - M\big(1-\xi_{ji}\big) \le 0 \tag{24}$$

$$\xi_{ij} \in \{0,1\} \tag{25}$$

where M is a sufficiently large positive number. Equation (19) constrains the restoration status and direction of transmission lines, (20) and (21) constrain each blackout bus to be restored by at most one available transmission line, (22) assigns large positive values for restoration time intervals of non-restored buses, and (23) and (24) calculate the restoration time intervals based on restoration directions and the required time of restoration operations, respectively.

Moreover, power flow constraints should be taken into consideration to achieve a feasible PSR solution. An ancillary variable $P_{i,t}^{G*}$ is introduced in the power flow equations to denote the active power generation of generating units. The linearized AC power flow proposed in [32] is adopted to calculate the power flows during the restoration process, and is described as follows to accommodate the time-varying network topologies during the PSR.

$$P_{i,t}^{\mathrm{G}*} - P_{i,t}^{\mathrm{G}} \le 0 \tag{26}$$

$$P_{i,t} = P_{i,t}^{\mathrm{G}*} - P_{i,t}^{\mathrm{L}} = \textstyle\sum_{ij\in\Omega_{\mathrm{L}}} P_{ij,t} \tag{27}$$

$$Q_{i,t} = Q_{i,t}^{\mathrm{G}} - Q_{i,t}^{\mathrm{L}} = \textstyle\sum_{ij\in\Omega_{\mathrm{L}}} Q_{ij,t} \tag{28}$$

$$P_{ij,t} + \varphi_{ij,t}^{\mathrm{p}} = g_{ij}(V_{i,t} - V_{j,t}) - b_{ij}(\theta_{i,t} - \theta_{j,t}) \tag{29}$$

$$Q_{ij,t} + \varphi_{ij,t}^{\mathrm{q}} = -b_{ij}\big(V_{i,t} - V_{j,t}\big) - g_{ij}\big(\theta_{i,t} - \theta_{j,t}\big) - \tfrac{b_{ij}^{\mathrm{lc}}}{2} V_{i,t} \tag{30}$$

$$-(1-\gamma_{ij,t})M \le \varphi_{ij,t}^{\mathrm{p}} \le (1-\gamma_{ij,t})M \tag{31}$$

$$-(1-\gamma_{ij,t})M \le \varphi_{ij,t}^{\mathrm{q}} \le (1-\gamma_{ij,t})M \tag{32}$$

$$-\gamma_{ij,t}P_{ij}^{\max} \le P_{ij,t} \le \gamma_{ij,t}P_{ij}^{\max} \tag{33}$$

$$-\gamma_{ij,t}Q_{ij}^{\max} \le Q_{ij,t} \le \gamma_{ij,t}Q_{ij}^{\max} \tag{34}$$

$$\gamma_{ij,t} - (\xi_{ij} + \xi_{ji}) \le 0 \tag{35}$$

$$\gamma_{ij,t} - \alpha_{i,t} \le 0\,, \gamma_{ij,t} - \alpha_{j,t} \le 0 \tag{36}$$

$$\alpha_{j,t} + \alpha_{i,t} + (\xi_{ij} + \xi_{ji}) - 2 - \gamma_{ij,t} \le 0 \tag{37}$$

$$V_i^{\min} \le V_{i,t} \le V_i^{\max} \tag{38}$$

$$\gamma_{ij,t} \in \{0,1\} \tag{39}$$

Equation (26) constrains the ancillary variable $P_{i,t}^{\mathrm{G}*}$ so it does not exceed the generation capacity $P_{i,t}^{\mathrm{G}}$. For RESs and conventional BSUs, $P_{i,t}^{\mathrm{G}}$ respectively denote the forecasted generation capacity at time slot *t* and rating capacity. For NBSUs, $P_{i,t}^{\mathrm{G}}$ is constrained by (10)-(13). The nodal power balance equations are expressed by (27) and (28). Equations (29) and (30) represent linearized power flow equations considering nodal voltage magnitudes and phase angles, (31) and (32) relax branch flow equations (29) and (30) by relaxing the ancillary variables $\varphi_{ij,t}^{\mathrm{p}}$ and $\varphi_{ij,t}^{\mathrm{q}}$ if the branch is not restored at time slot *t* (i.e., $\gamma_{ij,t} = 0$), respectively. Equations (33) and (34) constrain the active and reactive branch flow based on the capacity and on/off status of power lines, respectively. Equations (35)-(37) constrain the binary variable $\gamma_{ij,t}$, which indicates the on-off status of transmission line *ij* at time slot *t* (note that, based on (35)-(37), $\gamma_{ij,t}$ cannot be positive at time slot *t* unless the corresponding line *ij* and both terminal buses *i* and *j* are restored). Equation (38) constrains the nodal voltage magnitudes during the PSR process.

Constraints (26)-(39) are simplified from nonlinear AC power flow constraints. The effectiveness and accuracy of the adopted linearized AC power flow have been extensively investigated in [33] and thus will not be further discussed herein. Note that the linearized AC power flow (26)-(39) does not take the power loss into account. This is because the restored power loads during the first two PSR stages, i.e., the start-up of NBSUs and the formulation of restoration networks, are generally very small. Moreover, PSR studies the restoration of high-voltage transmission systems whose power loss is small even under nominal operating conditions. Thus, limited load consumption at these two PSR stages leads to a low level of power loss, and it is feasible to implement the lossless linearized AC power flow in the proposed PSR study.

In summary, the proposed integrated PSR model consists of the objective function (9) and constraints (10)-(39), and is denoted as the full model (FM).

B. Reformulated Model

The FM developed in the previous subsection is comprehensive as it integrates all the steady-state constraints in the generator startup and network reconfiguration stages. At the same time, solving the FM could be time-consuming. If it takes too long to solve the PSR model, the short-term RES forecasts discussed in Section III-D become out of date and errors cannot be neglected. To effectively utilize the short-term forecasts of RESs and timely support system operators make case-sensitive PSR decisions after a blackout, it is necessary to explore the possibility to reformulate the FM model and accelerate the solution speed.

The power flow constraints proposed in (26)-(39) are complex because the topology of the restored system is dynamic and varies with time. The power flow constraints are employed to guarantee that: 1) for any NBSU to be cranked, there exists an energized transmission path with sufficient capacity so that the required cranking power can be delivered, and 2) the active and reactive power of each restoration island can be balanced throughout the entire PSR process so that the operating constraints of power systems can be accommodated. The task of constructing a reformulated model (RM) is to simplify constraints (26)-(39) while maintaining the abovementioned two functions.

To simplify constraints (26)-(39), it is assumed that the active power loads are generally very small at the beginning of a PSR process and thus the transmission lines and transformers are lightly loaded. This assumption is valid and widely adopted in existing works such as [9], [17], [21]. Under this assumption, the major concern associated with constraints (26)-(39) is the excessive capacitive reactive power consumption caused by the energizing of light loaded transmission lines. The worst-case scenario is identified where no power loads are restored, and the restoration of no-load lines will result in the largest amount of capacitive reactive power consumption. As a result, if the PSR solution is able to balance the active and reactive power in each restoration island under the worst-case scenario, the power flow constraints (26)-(39) in the FM should be accommodated as well. Here, the power flow constraints (26)-(39) is modified to (40)-(45), where the active and reactive power balances at each restoration island throughout the PSR process are guaranteed.

$$P_{i,t} - \sum_{ij\in\Omega_{\mathrm{L}}} P_{ij,t} = 0 \tag{40}$$

$$Q_{i,t} + \Delta Q_{i,t}^{\mathrm{lc}} - \sum_{ij\in\Omega_{\mathrm{L}}} Q_{ij,t} = 0 \tag{41}$$

$$\left(\alpha_{i,t} + \xi_{ij} - 1\right) b_{ij}^{\mathrm{lc}} (V_i^{\max})^2 + \Delta Q_{i,t}^{\mathrm{lc}} \le 0 \tag{42}$$

$$\Delta Q_{i,t}^{\mathrm{lc}} \le 0 \tag{43}$$

$$-\xi_{ij} P_{ij}^{\max} \le P_{ij,t} \le \xi_{ij} P_{ij}^{\max} \tag{44}$$

$$-\xi_{ij} Q_{ij}^{\max} \le Q_{ij,t} \le \xi_{ij} Q_{ij}^{\max} \tag{45}$$

Equations (40) and (41) are respectively derived from (27) and (28) to balance the nodal active and reactive power injection. A new variable $\Delta Q_{i,t}^{\mathrm{lc}}$ denoting the reactive power associated with the charging of light loaded transmission lines is introduced to (41). Equations (42) and (43) calculate the reactive power of transmission line charging capacitors ($\Delta Q_{i,t}^{\mathrm{lc}}$) based on restoration operations, and (44) and (45) constrain the line flows with respect to the restoration decisions, respectively.

Note that special emphasis is given to the balance of reactive power in (40)-(45). The introduced $\Delta Q_{i,t}^{\mathrm{lc}}$ represents the increment of reactive power due to the restoration of transmission lines. For transmission lines, $b_{ij} \gg b_{ij}^{\mathrm{lc}}$ generally holds. Thus, the increment of reactive power injection ΔQ_i^{lc} at bus *i* due to the restoration of line *ij* can be approximated by (46).

$$\begin{aligned}\Delta Q_i^{\mathrm{lc}} &= -\frac{1}{2} b_{ij}^{\mathrm{lc}} \left|V_{i,t}\right|^2 - \frac{1}{2} b_{ij}^{\mathrm{lc}} \frac{g_{ij}^2 + b_{ij}(b_{ij} + b_{ij}^{\mathrm{lc}}/2)}{g_{ij}^2 + \left(b_{ij} + b_{ij}^{\mathrm{lc}}/2\right)^2} \left|V_{i,t}\right|^2 \\ &\approx -b_{ij}^{\mathrm{lc}} \left|V_{i,t}\right|^2 \ge -b_{ij}^{lc} (V_i^{\max})^2 \end{aligned} \tag{46}$$

The approximation (46) is adopted to formulate (42). Because (46) overestimates the reactive power increment caused by restoration operations, the feasible solution based on reformulated constraints (40)-(45) will always satisfy the original constraints (26)-(39).

Furthermore, the original generator startup constraints (10)-(18) utilize two sets of binary variables, $\alpha_{i,t}$ and $\beta_{i,t}$, to represent the startup and ramping status of NBSUs. Because τ_i^{st} is a constant value for any NBSU, either $\alpha_{i,t}$ or $\beta_{i,t}$ can be relaxed as a continuous variable. The following reformulations (47) and (48) are adopted to modify (16) and (17) so that $\alpha_{i,t}$ can be relaxed by a continuous variable $\bar{\alpha}_{i,t}$:

$$\tau_i^{\mathrm{st}} + 1 = \sum_{k=t-\tau_i^{\mathrm{st}}-1} \bar{\alpha}_{i,t} - \sum_{k=t} \beta_{i,k} \tag{47}$$

$$\beta_{i,t} \le \bar{\alpha}_{i,t} \le 1 \tag{48}$$

where (47) and (48) together guarantee the continuous variable $\bar{\alpha}_{i,t}$ has exactly the same value as $\alpha_{i,t}$ based on constraints (16) and (17). By doing so, the number of binary variables in constraints (10)-(18) is reduced by half.

V. Integrating Availability Assessment and Power System Restoration Models

The constraints of short-term RES forecasts (i.e., (6)-(8)) can directly apply to the mathematical models proposed in Section IV. On the other hand, the assessed availability of transmission components consists of different modules that should be combined before integrating into the PSR models.

Based on both offline and online assessments, the comprehensive availability of a certain facility can be calculated by (49). The calculated ψ_x is case sensitive because it integrates the online assessment results f_x and s_x that are relevant to specific blackout cases. The integrated availability (represents the success rate) for restoring a set of facilities (denoted as $\Omega_{\mathrm{X}'}$) can be further calculated by (50).

$$\psi_x = r_x f_x s_x \tag{49}$$

$$\Psi_{\sum x} = \prod_{x\in\Omega_{\mathrm{X}'}} \psi_x \tag{50}$$

Equation (50) can be further simplified to (51), where ψ_x^- and $\Psi_{\sum x}^-$ are defined by $\psi_x^- = 1 - \psi_x$ and $\Psi_{\sum x}^- = 1 - \Psi_{\sum x}$, respectively. Because ψ_x and $\Psi_{\sum x}$ represent the success rate of restoring one and a certain number of facilities, ψ_x^- and $\Psi_{\sum x}^-$ can be regarded as risk measures of the corresponding restoration operations.

$$\Psi_{\sum x} = 1 - \Psi_{\sum x}^- \approx 1 - \sum_{x\in\Omega_{\mathrm{X}'}} \psi_x^- \tag{51}$$

The risk of restoring a blackout bus can be approximated as the cumulative risk of associated restoration operations using (51). For instance, to restore a blackout bus *i* from bus *j*, the risk of restoring line *ij* (ψ_{ij}^-) and bus *i* (ψ_i^-) should be summed to estimate the risk of this restoration operation. Similar to the calculation of restoration timing discussed in (19)-(25), the cumulative risk of restoring blackout buses can be obtained from (52)-(55).

$$\Psi_i^- = 0\,, \forall i \notin \Omega_{\mathrm{N}} \tag{52}$$

$$-\Psi_i^- \le 0 \tag{53}$$

$$\Psi_i^- - \Psi_j^- + \psi_{ij}^- + \psi_j^- - M\left(1 - \xi_{ij}\right) \le 0 \tag{54}$$

$$\Psi_j^- - \Psi_i^- + \psi_{ij}^- + \psi_i^- - M\left(1 - \xi_{ji}\right) \le 0 \tag{55}$$

Equation (52) assigns zero risks to buses in the non-blackout area, while the buses in the blackout area have non-negative risk measures according to (53). Equations (54) and (55) calculate the cumulative risk of restoring a certain blackout bus with respect to the direction of the restoration operation. If bus *i* is restored from bus *j* by energizing line *ij*, then the cumulative restoring risk of bus *i* (Ψ_i^-) equals the summation of cumulative risk of bus *j* (Ψ_j^-), ψ_{ij}^-, and ψ_i^-.

As the availability assessments illustrate the success rate of restoration decisions, they should be integrated into the proposed FM and RM. The expectations of restored generation capacities will be adopted to replace original objective function (9) as shown in (56). However, the objective function (56) contains a bilinear term $\Psi_i^-(P_{i,t}^{\mathrm{G}} - P_{i,t}^{\mathrm{L}})$, which will significantly increase the computational burden. In this paper, the parameter P_i^{set} is employed to replace the variable $P_{i,t}^{\mathrm{G}} - P_{i,t}^{\mathrm{L}}$ in the bilinear term, and a non-negative risk factor π is introduced to represent the risk preference of system operators. Thus, (56) can be reformulated as (57).

$$\mathrm{Max}\ \ \sum_{i\in\Omega_{\mathrm{N}}}\sum_{t\in\Omega_{\mathrm{T}}}(1-\Psi_i^-)(P_{i,t}^{\mathrm{G}}-P_{i,t}^{\mathrm{L}}) \tag{56}$$

$$\mathrm{Max}\ \ \sum_{i\in\Omega_{\mathrm{N}}}\sum_{t\in\Omega_{\mathrm{T}}}(P_{i,t}^{\mathrm{G}}-P_{i,t}^{\mathrm{L}})-\sum_{i\in\Omega_{\mathrm{N}}}\pi\Psi_i^-\,P_i^{\mathrm{set}} \tag{57}$$

By using modified objective function (57), the proposed PSR models, i.e., FM and RM, are categorized as MILP models. Table I summarizes and compares the characteristics of the proposed FM and RM. The number of binary variables is significantly reduced based on the proposed reformulation. Thus, RM is expected to be superior to the FM in terms of computational efficiency.

TABLE I
COMPARISON OF PROPOSED FULL PSR MODEL AND REFORMULATED MODEL

	FM	RM
Objective	(57)	(57)
Constraints	(6)-(8), (10)-(39), (52)-(55)	(6)-(8), (10)-(15), (19)-(25), (40)-(45), (47)-(48), (52)-(55)
Number of binary variables	$2N_{\mathrm{B}}N_{\mathrm{T}}+2N_{\mathrm{L}}+N_{\mathrm{L}}N_{\mathrm{T}}$	$N_{\mathrm{B}}N_{\mathrm{T}}+2N_{\mathrm{L}}$

VI. CASE STUDIES

A. Test Systems Descriptions

In this section, the following two test systems are employed to validate the effectiveness of the proposed PSR models:

1. The standard IEEE 118-bus test system with 19 generating units, 118 buses, and 186 transmission lines [34].
2. An actual power system in Guangzhou, China. This system contains 29 generating units, 162 buses, and 212 transmission lines [21].

The proposed models are solved by GAMS/CPLEX solver on a desktop computer with an Intel i7-7700 processor and 12 GB RAM. The blackouts are assumed to occur at time t=0 min, the required restoration time $\Delta\tau_{ij}$ for power lines and the length of the time slot are set to 10 min, and a total time span of 5 hours is considered (30 time slots in total). Each device in the outage area is assigned a randomly generated value ranging from 99 to 100% to represent the reliability (r_x). Parameters π, ω, and $\varepsilon_{x,y}$ are set to 5, 0.8, and 4.6, respectively. The assigned values of ω, and $\varepsilon_{x,y}$ are discussed in Section III, and the influences of π will be demonstrated in the case studies.

B. A Regional Blackout in the IEEE 118-bus System

A regional blackout is introduced to the IEEE 118 bus system with the non-outage area, severe weather-affected area (lightly & dark shaded), and initial fault area (dark shaded) as illustrated in Fig. 5. Four connection lines, namely 15-33, 19-34, 23-24, and 30-38, connect the non-outage area to the blackout area. In addition to the proposed models, a mathematical programming-based method B-1 [8] and a graph theory-based method B-2 [12] are selected as benchmarks. Lines 69-75 and 69-77 are assumed to be diagnosed as actual fault (fault signs in Fig. 5) lines and the $v_{x,y}$ of facilities in the severe weather-affected area are randomly assigned values ranging from ($v_{x,y}^{\mathrm{std}}$,1.25$v_{x,y}^{\mathrm{std}}$]. The following cases are simulated:

Case I: PSR without availability assessment.

Case II: PSR with availability assessment.

The optimized PSR solutions in these two cases are indicated by solid lines in Fig. 5. The proposed FM, RM, and benchmarks B-1 and B-2 result in the same PSR solution in Case I, as demonstrated by solid lines in Fig. 5(a). With availability assessment module discussed in Section III integrated into the proposed PSR model, the optimized PSR solution is demonstrated by Fig. 5(b). Because availability assessment cannot be integrated into models in B-1 and B-2, their optimized PSR solutions remain the same as shown in Fig. 5(a). The CPU times of FM and RM to solve Case I (Case II) are 20160.7 s and 826.2 s (19811.4 s and 861.6 s), respectively.

In Fig. 5(a), two parallel restoration paths are generated starting from lines 23-24 and 30-38. But, the absence of an availability assessment leads to the restoration of faulted line 69-77 in Fig. 5(a). In Fig. 5(b), in which the availability assessment is considered, three parallel restoration paths are generated starting from lines 15-33, 19-34, and 30-38, and neither faulted lines are restored. As can be observed from Fig. 5, the restoration of certain buses and lines in the severe weather-affected area are inevitable to crank the NBSUs at buses 46 and 49. Table II lists the restoration results of buses and lines in the severe weather-affected area (lightly & dark shaded) of both Cases I and II. Note that only the differences in the results between Cases I and II are shown while the common parts are not shown. The average assessed availability against severe weather (s_x) of restored buses and lines in Case I (Case II) are 0.461 and 0.535 (0.469 and 0.750), respectively. With the proposed availability assessment taken into account, the devices (especially the transmission lines) selected to be restored in Case II generally have higher probabilities to withstand the negative impacts of severe weather. Thus, the integration of availability assessment into PSR models is very crucial to identify vulnerable devices and alleviate restoration risks, especially in cases of weather-related blackouts.

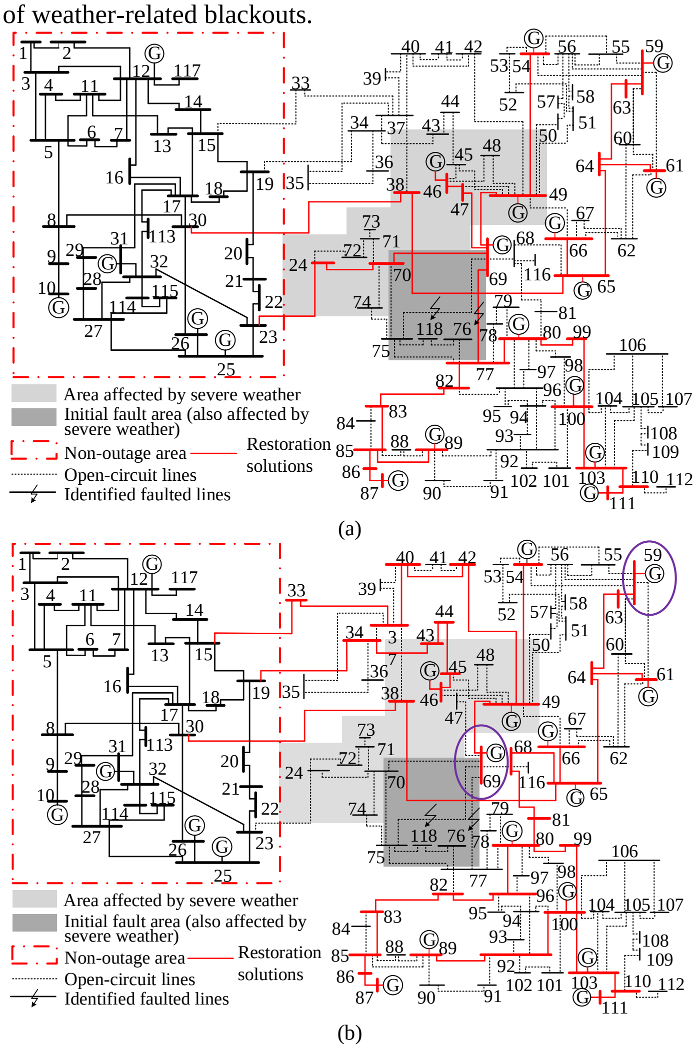

Fig. 5. IEEE 118 bus test system and simulated regional blackout: (a) PSR without availability assessment (Case I), (b) PSR with availability assessment (Case II).

TABLE II
DIFFERENCES IN PSR SOLUTIONS IN SEVERE WEATHER AFFECTED AREA BETWEEN CASES I AND II

	Restored buses (s_x)	Restored lines (s_x)
Case I	24 (0.549), 47 (0.398), 70 (0.436)	23-24 (0.387), 24-70 (0.858), 69-70 (0.470), 46-47 (0.569), 47-69 (0.486), 69-77 (0.441)
Case II	43 (0.551), 45 (0.387)	34-43 (0.982), 43-44 (0.323), 44-45 (0.825), 45-46 (0.885), 42-49 (0.734)

TABLE III
RESTORATION OF NBSU AT BUS 69

Solution	Restoration path	Restoration time (min)	Assessed risk Ψ_{69}^{-}	Actual success rate Ψ_{69}
Optimized	49-69	60	0.689	43.2%
Alternative	68-69	40	1.225	19.9%
	23-24-70-69	30	2.317	3.6%

TABLE IV
RESTORATION OF NBSU AT BUS 59

Solution	Restoration path	Restoration time (min)	Assessed risk Ψ_{59}^{-}	Actual success rate Ψ_{59}
Optimized	63-59	50	1.245	26.2%
Alternative	54-59	70	1.085	28.7%

TABLE V
THE IMPACT OF RISK PREFERENCE π

π	Highest Ψ_i^{-} (NBSU bus)	Latest cranking time (NBSU bus)
0	4.399 (46)	100 min (111)
1	3.315 (46)	100 min (111)
5	2.670 (46)	110 min (87)
10	2.356 (46)	150 min (87)
15	2.356 (46)	150 min (87)

Tables III and IV compare the optimized restoration paths (shown in Fig. 5(b)) and alternative restoration paths (obtained from the topology information) to crank buses 69 and 59 (ellipses in Fig. 5(b)), respectively. According to Table III, bus 69 is restored at 60 min with an assessed risk of 0.689. Two alternative restoration paths that may restore bus 69 at earlier times are not selected, as those paths lead to higher risks (1.225 and 2.317, respectively). Judging from $\Psi_{\sum x}$ which accurately evaluates the success rate, restoring bus 69 through the optimized path has a success rate of 43.2% which is much higher than those of the alternative paths (19.9% and 3.6%, respectively). On the contrary, Table IV shows that path 63-59 is selected instead of path 54-59 to restore bus 59. The assessed risk and the actual success rate of the former path are respectively 1.245 and 26.2%. Although the alternative path has a lower risk and higher success rate (1.085 and 28.7%, respectively), it is not selected by the proposed model because the alternative path will postpone the restoration of bus 59 by 20 minutes. In addition, the effectiveness of the proposed risk approximation method in Section V is also validated because the restoration operations with higher assessed risks have lower success rates (i.e., higher Ψ_i^{-} indicates lower $\Psi_{\sum x}$).

The reason that Tables III and IV demonstrate the opposite results roots in the value of the selected risk factor π. Based on the default risk factor ($\pi = 5$), the optimized restoration paths outweigh the alternative solutions in terms of balancing the risk management and restoration speed during the PSR process. The risk preference can be adjusted by modifying the value of π. Table V lists the highest Ψ_i^{-} and latest cranking time of NBSUs with various π, and clearly demonstrates that the optimized restoration strategy is more risk-averse and time-consuming with higher π. System operators can obtain PSR solutions with various risk preferences by adjusting π to accommodate the conditions of specific blackouts.

C. A Global Blackout in the IEEE-118-bus system with RESs

A global blackout scenario is simulated in this section. In the system studied, a conventional BSU located at bus 26 and two wind farms respectively located at buses 61 and 89 functions as BSUs (ellipses in Fig. 6). The optimized PSR solutions are indicated by *solid red* lines in Fig. 6. The CPU times of FM and RM to solve the global blackout scenario are 8481.5 s and 316.1 s, respectively.

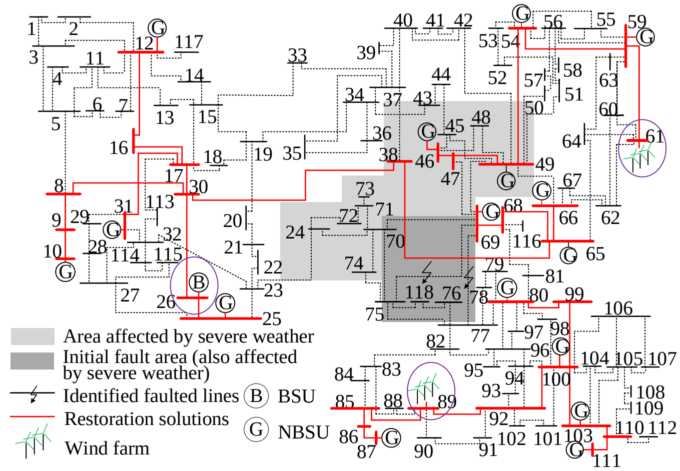

Fig. 6. Optimized PSR in the global blackout scenario with RESs.

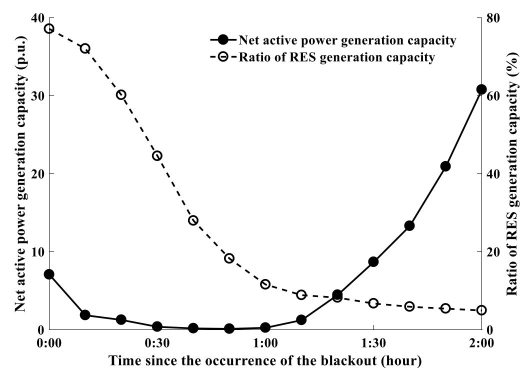

Fig. 7. Profiles of the net active generation capacity and the ratio of RES generation capacity during the first two hours of the PSR.

Fig. 6 shows that three restoration islands are formulated in the global blackout scenario because there are three units with black-start capability. To investigate the influences of renewable wind farms on the PSR process, the net active generation capacity (i.e., $P_{i,t}^{\mathrm{G}} - P_{i,t}^{\mathrm{L}}$) and the ratio of RES generation capacity in the total generation capacity during the first two hours of the PSR process are demonstrated in Fig. 7. At the beginning of the PSR process, BSUs must supply cranking power to the NBSUs, thus the net active power capacity gradually decreases in the first hour in Fig. 7. During this period when the error in short-term generation forecasts is very small, the proposed PSR model is able to effectively utilize the forecasted RES generation capacity and deploy the RESs as the major source of power supply. As the PSR process proceeds, the net active power capacity grows rapidly thanks to the ramping of restored NBSUs. Hence, the share of RES capacity in the total generation capacity drops significantly. Although larger RES generation forecast error may occur as the PSR process proceeds, the restored system already has sufficient generation capacity to deal with the uncertainty and fluctuation of RESs.

In summary, employing short-term RES generation forecasts is a feasible solution to handle RESs during the PSR process.

D. A Global Blackout in an Actual Power System with RESs

A global blackout in an actual power system in Guangzhou, China, is employed to verify the effectiveness of the proposed PSR models considering the integration of RESs. The studied system has three BSUs, i.e., a conventional BSU located at bus 9 and two wind farms respectively located at buses 88 and 121. Without loss of generality, the generation forecast of the wind farm at bus 88 (121) is assumed to be higher (lower) than its typical generation outputs after the occurrence of the blackout. Two scenarios (named as scenarios S1 and S2) with different weather-affected areas and faulted devices are simulated, and the optimized PSR solutions of RM are indicated by *solid red* lines in Fig. 8. The average CPU times of FM and RM to solve these two scenarios are 10390.1 s and 278.3 s, respectively.

Fig. 8 shows that three restoration islands are formulated in both scenarios. The proposed models will clearly generate different PSR solutions that are sensitive to the diagnosed faults and the weather-affected area. Unlike the simulation results in Section VI-B and VI-C where all the NBSUs are restored, at least one NBSU located in the severe weather-affected areas is not restored in both Figs. 8(a) and 8(b). Although these NBSUs can be cranked through lines that have not suffered from faults, the restoration risks associated with the severe weather are the primary reason that they are not included in the optimized PSR solutions.

Table VI is introduced to compare the proposed case-sensitive PSR solution in the simulated scenario in Fig. 8(a) with conventional PSR planning models that utilize stochastic optimization to model the uncertainty of RESs [21]. Because the wind farm at bus 88 (121) has a higher (lower) short-term generation forecast, the proposed case-sensitive PSR solution is quite different from that obtained from conventional models that utilize historical data and probability distributions to estimate the generation profiles of RESs. According to the solution to the conventional PSR model, NBSUs at buses 111, 114, and 138 will be restored by the wind farm at bus 121, while the proposed case-sensitive PSR solution clusters these NBSUs into the restoration island of the wind farm at bus 88. Table VI shows the NBSUs generally enjoy a faster recovery speed based on the proposed case-sensitive PSR solution as the forecast for RESs are more accurate. Although the startup of the NBSU at bus 138 is accelerated based on the case-insensitive solution, the restoration of other NBSUs will be postponed due to the scarce generation capacity of RES at bus 121.

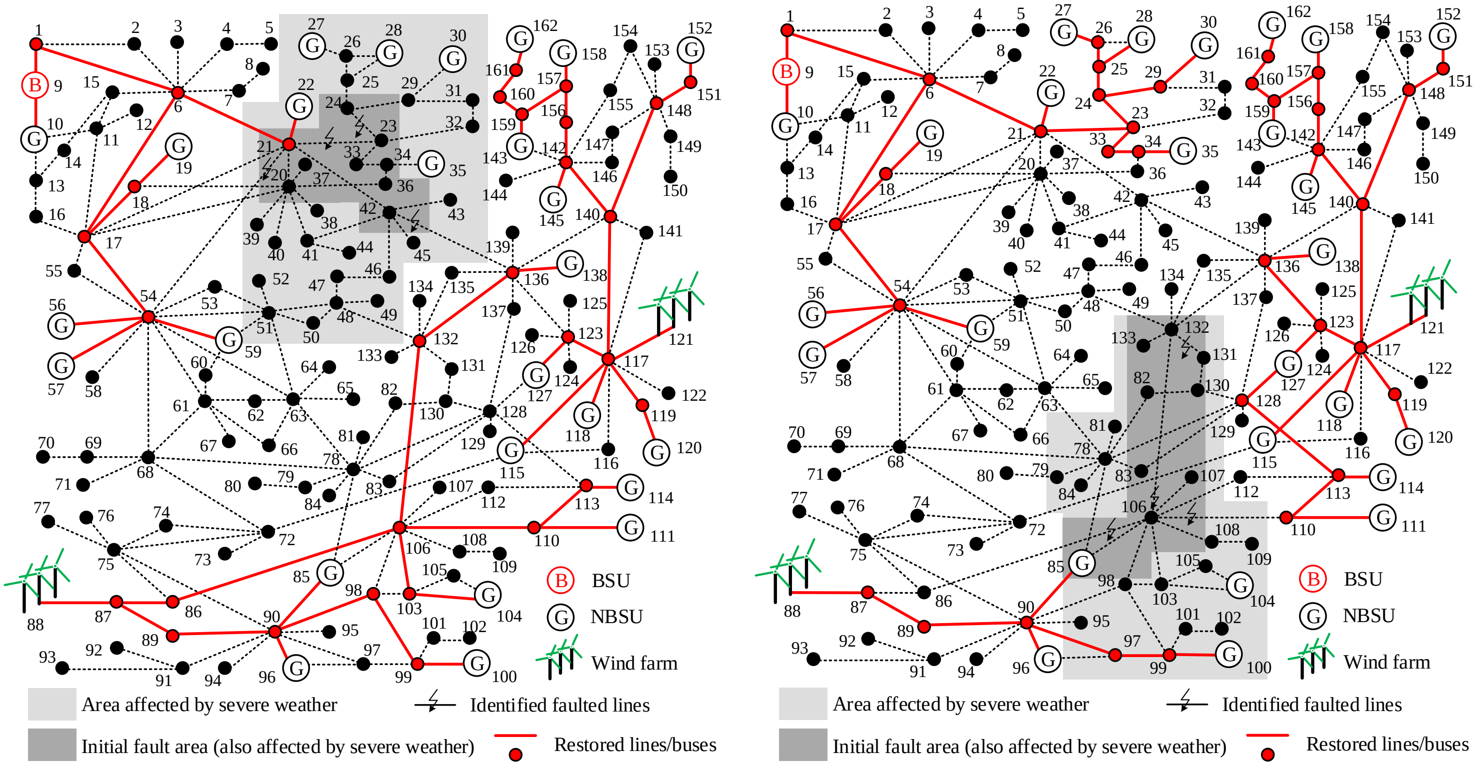

Fig. 8. Simulated restoration solutions of an actual power system with renewables: (a) scenario S1. (b) scenario S2.

TABLE VI
NBSU CRANKING TIME COMPARISON WITH RESS FOR SCENARIO S1

	Proposed case-sensitive solution	Case-insensitive solution based on [21]
NBSU at bus 111	60 min	110 min
NBSU at bus 114	80 min	100 min
NBSU at bus 138	70 min	60 min
Average cranking time of all restored NBSUs	56.8 min	63.2 min

E. Discussions

Although the impact of severe weather is emphasized in this paper, the proposed PSR also works for other situations without severe weather. The proposed availability assessment in Section III consists of three parts: reliability, fault diagnosis, and impact of severe weather. If a blackout is not caused by the severe weather, the assessed availability of buses/lines is mainly influenced by the historical reliability performance and the fault diagnosis results. For non-weather-related blackouts, the proposed availability assessment method and the PSR model do not need to be modified and the PSR solution will be automatically optimized. If the blackout is not associated with physical damages on the transmission components, the case-sensitive PSR method is not different from other existing methods. However, we wish to emphasize that the generator startup and network formulation should remain integrated when the transmission components are not damaged. During the restoration, the power flow constraints can be violated due to the high voltage issues caused by restoring light-loaded transmission lines. Using methods such as [8] and [12], the feasibility check will reject the generator startup results, but the convergence of these optimization-feasibility check process is not guaranteed.

Observed from the simulation results in Sections VI-C and VI-D, several islands are formulated as restoration subsystems. These islands are capable of accelerating the cranking of NBSUs while minimizing the energizing of transmission lines/substations to avoid risks. On the other hand, the islanded operation is challenged by stability concerns such as frequency issues and voltage issues, especially when the black-start sources are renewable energy sources. The frequency issue is mainly caused by the generation forecast error of renewable energy sources. Because the proposed PSR is case-sensitive and is optimized after the blackout, the highly accurate short-term forecast is employed to handle the first factor and the effectiveness is validated in Section VI-C. Moreover, the integration of energy storage system is another viable solution as discussed in Section III-D.

The voltage issue during restoration stage is normally caused by the energizing of light-loaded transmission lines. The inverters of renewable energy sources can provide flexible reactive power support (both consumption and generation) utilizing the capacity of the inverters. In addition, the reactive power is usually locally compensated in bulk power systems, and the reactive power flow and reactive power balance have been properly considered in the proposed PSR models in Section IV. Thus, the islanded restoration subsystems with renewables will not cause significant voltage issues as discussed in [19].

According to the simulation results, it takes hours to obtain a PSR solution based on the FM, which is not feasible for real-world application because the case-sensitive PSR models are solved after the blackout occurs. The RM can be solved in several minutes, which is much faster than FM. With the improved computational efficiency, the short-term RES forecasts are still valid to be employed in the RM. Considering the fact that the system operators have to spend some time restarting the black-start units before initiating the PSR operations, the RM is computationally efficient to provide case-sensitive PSR solutions to support the decision-making of system operators during restoration.

VII. Conclusions

This paper proposes a case-sensitive PSR method for bulk power systems that integrates the startup of NBSUs, the formulation of a restoration network, and the evaluated availability of equipment. The availability of transmission components after blackouts is assessed based on both offline reliability data and online fault diagnosis and weather data. An integrated PSR model (FM) is proposed to integrate the NBSU startup optimization and network topology formulation. To accommodate the short-term RES generation forecasts, a reformulated model (RM) is developed to accelerate the computational speed. The assessed availability is further integrated into both the FM and RM to generate case-sensitive PSR solutions after blackouts.

The effectiveness of the proposed models in optimizing case-sensitive PSR solutions has been verified in case studies. Compared to existing studies, the proposed methods are sensitive to the features of blackout scenarios and can steer clear from components with high risks. Simulation results have also validated that the reformulated PSR model can be solved in minutes, making the implementation of short-term RES generation forecasts feasible in optimizing case-sensitive PSR solutions for blackout power systems with RESs.

References

[1] F. Qiu and P. Li, “An integrated approach for power system restoration planning,” *Proc. IEEE*, vol. 105, no. 7, pp. 1234-1252, Jul. 2017.

[2] C. Chen, J. Wang, F. Qiu, and D. Zhao, “Resilient distribution system by microgrids formation after natural disasters,” *IEEE Trans. Smart Grid*, vol. 7, no. 2, pp. 958-966, Mar. 2016.

[3] U.S. Executive Office of the President, “Economic benefits of increasing electric grid resilience to weather outages.” Aug. 2013. [Online]. Available: https://www.energy.gov/sites/prod/files/2013/08/f2/Grid%20Resiliency%20 Report_FINAL.pdf

[4] Q. Chen, X. Yin, D. You, H. Hou, G. Tong, B. Wang, and H. Liu, “Review on blackout process in China southern area main power grid in 2008 snow disaster,” in *IEEE PES General Meeting*, Calgary, AB, Canada, Jul. 2009.

[5] N. Abi-Samra, J. McConnach, S. Mukhopadhyay, and B. Wojszczyk, “When the bough breaks: Managing extreme weather events affecting electrical power grids,” *IEEE Power Energy Mag.*, vol. 12, no. 5, pp. 61–65, Sep./Oct. 2014.

[6] R. Yan, N.-A. Masood, T. K. Saha, F. Bai, and H. Gu, “The anatomy of the 2016 South Australia blackout: a catastrophic event in a high renewable network,” *IEEE Trans. Power Syst.*, vol. 33, no. 5, pp. 5374-5388, Sep. 2018.

[7] W. J. Liu, Z. Z. Lin, F. S. Wen, and G. Ledwich, “Intuitionistic fuzzy Choquet integral operator-based approach for black-start decision-making,” *IET Gener. Transm. Distrib.*, vol. 6, no. 5, pp. 378-386, May 2012.

[8] W. Sun, C.-C. Liu, and L. Zhang, “Optimal generator start-up strategy for bulk power system restoration,” *IEEE Trans. Power Syst.*, vol. 26, no. 3, pp. 1357-1366, Aug. 2011.

[9] X. Gu, W. Liu, and C. Sun, “Optimisation for unit restarting sequence considering decreasing trend of unit start-up efficiency after a power system blackout,” *IET Gener. Transm. Distrib.*, vol. 10, no. 16, pp. 4187-4196, Dec. 2016.

[10] F. Qiu, J. Wang, C. Chen, and J. Tong, “Optimal black start resource allocation,” *IEEE Trans. Power Syst.*, vol. 31, no. 3, pp. 2493-2494, May 2016.

[11] C. Wang, V. Vittal, and K. Sun, “OBDD-based sectionalizing strategies for parallel power system restoration,” *IEEE Trans. Power Syst.*, vol. 26, no. 3, pp. 1426-1433, Aug. 2011.

[12] Z. Lin, F. Wen, and Y. Xue, “A restorative self-healing algorithm for transmission systems based on complex network theory,” *IEEE Trans. Smart Grid*, vol. 7, no. 4, pp. 2154-2162, Jul. 2016.

[13] J. Li, X. Y. Ma, C. C. Liu, and K. P. Schneider, “Distribution system restoration with microgrids using spanning tree search,” *IEEE Trans. Power Syst.*, vol. 29, no. 6, pp. 3021-3029, Nov. 2014.

[14] B. Chen, C. Chen, J. Wang, and K. L. Butler-Purry, “Sequential service restoration for unbalanced distribution systems and microgrids,” *IEEE Trans. Power Syst.*, vol. 33, no. 2, pp. 1507-1520, Mar. 2018.

[15] W. Liu, Z. Lin, F. Wen, and G. Ledwich, “A wide area monitoring system based load restoration method,” *IEEE Trans. Power Syst.*, vol. 28, no. 2, pp. 2025-2034, May 2013.

[16] H. Gao, Y. Chen, Y. Xu, and C. C. Liu, “Resilience-oriented critical load restoration using microgrids in distribution systems,” *IEEE Trans. Smart Grid*, vol. 7, no. 6, pp. 2837-2848, Nov. 2016.

[17] Y. Hou, C. C. Liu, K. Sun, P. Zheng, S. Liu, and D. Mizumura, “Computation of milestones for decision support during system restoration,” *IEEE Trans. Power Syst.*, vol. 26, no. 3, pp. 1399-1409, Aug. 2011.

[18] A. Golshani, W. Sun, Q. Zhou, Q. P. Zheng, and J. Tong, “Two-stage adaptive restoration decision support system for a self-healing power grid,” *IEEE Trans. Ind. Informat.*, vol. 13, no. 6, pp. 2802-2812, Dec. 2017.

[19] L. Sun, C. Peng, J. Hu, and Y. Hou, “Application of type 3 wind turbines for system restoration,” *IEEE Trans. Power Syst.*, vol. 33, no. 3, pp. 3040-3051, May 2018.

[20] A. Golshani, W. Sun, Q. Zhou, Q. P. Zheng, and Y. Hou, “Incorporating wind energy in power system restoration planning,” *IEEE Trans. Smart Grid*, vol. 10, no. 1, pp. 16-28, Jan. 2019.

[21] L. Sun, W. Liu, C. Y. Chung, M. Ding, R. Bi, and L. Wang, “Improving the restorability of bulk power systems with the implementation of a WF-BESS system,” *IEEE Trans. Power Syst.*, vol. 34, no. 3, pp. 2366-2377, May 2019.

[22] ANSI/IEEE Standard 762-2006, “IEEE Standard Definitions for Use in Reporting Electric Generating Unit Reliability, Availability, and Productivity,” Dec. 2006.

[23] Reliability Test System Task Force, “The IEEE reliability test system 1996,” *IEEE Trans. Power Syst.*, vol. 14, no. 3, pp. 1010-1020, Aug. 1999.

[24] Y. Zhang, C. Y. Chung, F. Wen, and J. Zhong, “An analytic model for fault diagnosis in power systems utilizing redundancy and temporal information of alarm messages,” *IEEE Trans. Power Syst.*, vol. 31, no. 6, pp. 4877-4886, Nov. 2016.

[25] W. Guo, F. Wen, G. Ledwich, Z. Liao, X. He, and J. Liang, “An analytic model for fault diagnosis in power systems considering malfunctions of protective relays and circuit breakers,” *IEEE Trans. Power Del.*, vol. 25, no. 3, pp. 1393-1401, Jul. 2010.

[26] H. Yang, C. Y. Chung, J. Zhao, and Z. Dong, “A probability model of ice storm damages to transmission facilities,” *IEEE Trans. Power Del.*, vol. 28, no. 2, pp. 557-565, Apr. 2013.

[27] W. Liu, L. Sun, Z. Lin, F. Wen, and Y. Xue, “Multi-objective restoration optimization of power systems with battery energy storage systems,” *IET Gener. Transm. Distrib.*, vol. 10, no. 7, pp. 1749-1757, Jul. 2016.

[28] N. Safari, C. Y. Chung, and G. C. D. Price, “Novel multi-step short-term wind power prediction framework based on chaotic time series analysis and singular

spectrum analysis," *IEEE Trans. Power Syst.*, vol. 33, no. 1, pp. 590-601, Jan. 2018.

[29] N. C. Koutsoukis, P. S. Georgilakis, and N. D. Hatziargyriou, "Multistage coordinated planning of active distribution networks," *IEEE Trans. Power Syst*., vol. 33, no. 1, pp. 32-44, Jan. 2018.

[30] B.-M. Hodge and M. Milligan, "Wind power forecasting error distributions over multiple timescales," in *IEEE PES General Meeting*, Detroit, MI, USA, Jul. 2011, 8p.

[31] G. Giebel, "The state of the art in short-term prediction of wind power," [Online]. Available: https://doi.org/10.11581/DTU:00000017

[32] H. Zhang, G. T. Heydt, V. Vittal, and J. Quintero, "An improved network model for transmission expansion planning considering reactive power and network losses," *IEEE Trans. Power Syst.*, vol. 28, no. 3, pp. 3471-3479, Aug. 2013.

[33] J. Yang, N. Zhang, C. Kang, and Q. Xia, "A state-independent linear power flow model with accurate estimation of voltage magnitude*," IEEE Trans. Power Syst.*, vol. 32, no. 5, pp. 3607-3617, Sep. 2017.

[34] A. Arab, A. Khodaei, S. K. Khator, K. Ding, V. A. Emesih, and Z. Han, 'Stochastic pre-hurricane restoration planning for electric power systems infrastructure,' *IEEE Trans. Smart Grid*, vol. 6, no. 2, pp. 1046-1054, Mar. 2015.

Weijia Liu received the B.Eng. and Ph.D. degrees in electrical engineering from Zhejiang University, Hangzhou, China, in 2011 and 2016, respectively.

He is currently a Researcher at Power System Engineering Center, National Renewable Energy Laboratory, Golden, CO, U.S.A.

Junpeng Zhan (M'16) received B.Eng. and Ph.D. degrees in electrical engineering from Zhejiang University, Hangzhou, China, in 2009 and 2014, respectively.

He is currently a Research Associate Electrical Engineer at Brookhaven National Laboratory, Upton, NY, U.S.A.

C. Y. Chung (M'01-SM'07-F'16) received the B.Eng. (with First Class Honors) and Ph.D. degrees in electrical engineering from The Hong Kong Polytechnic University, Hong Kong, China, in 1995 and 1999, respectively.

He is currently a Professor, the NSERC/SaskPower Senior Industrial Research Chair in Smart Grid Technologies, and the SaskPower Chair in Power Systems Engineering in the Department of Electrical and Computer Engineering at the University of Saskatchewan, Saskatoon, SK, Canada.

Dr. Chung is an Editor of *IEEE Transactions on Power Systems*, *IEEE Transactions on Sustainable Energy*, and *IEEE Power Engineering Letters*. He is also a member of the IEEE PES Fellow Evaluation Committee.

Lei Sun received the B.Eng. degree from East China University of Science and Technology, Shanghai, China, in 2012, and the Ph.D. degree from Zhejiang University, Hangzhou, China, in 2017, both in electrical engineering.

He is currently a lecturer in the School of Electrical Engineering and Automation, Hefei University of Technology, Hefei, China.